Microelectronics Reliability 59 (2016) 55–59

Contents lists available at ScienceDirect

Microelectronics Reliability

journal homepage: www.elsevier.com/locate/mr

Analysis of origin of measured 1/*f* noise in high-power semiconductor laser diodes far below threshold current

Jian Guan [a], Shuxu Guo [a], Jinyuan Wang [a,c], Min Tao [a], Junsheng Cao [b], Fengli Gao [a,*]

[a] State Key Laboratory on Integrated Optoelectronics, College of Electronic Science and Engineering, Jilin University, Changchun 130012, China
[b] Changchun Institute of Optics, Fine Mechanics and Physics, Chinese Academy of Sciences, Changchun 130033, China
[c] Department of Aviation Lifesaving Equipment, Aviation University Air Force, Changchun 130000, China

ARTICLE INFO

Article history:
Received 6 September 2015
Received in revised form 17 November 2015
Accepted 18 December 2015
Available online 29 December 2015

Keywords:
High-power semiconductor laser diodes
1/*f* noise
Electrical derivative
Reliability

ABSTRACT

The 1/*f* noise is measured under the bias one tenth the threshold current of the InGaAs quantum well high-power semiconductor laser diodes (LDs). The noise origin is analyzed using the current and voltage 1/*f* noise and dynamic resistance characteristics. Then the relationship between the noise and the internal defect is analyzed according to the differences of LDs in the noise intensity and the fluctuation near the initial electrical derivative peak. The result shows that with currents 0.13 mA–1 mA, the dynamic resistance of the LDs is in the magnitude of hundreds of ohms, when the changing rates of both the noise intensity and the resistance reflect the typical features of the active region, while with currents 8 mA–32 mA, the dynamic resistance drops under 10 Ω and its changing rate slows down, when the 1/*f* noise intensity trend shows the features of the contact resistance. Moreover, the electrical derivative of LDs with weaker noise fluctuates milder and has more conspicuous initial peaks, while the electrical derivative of other LDs fluctuates acuter and hardly shows distinct initial peaks. The results indicate that the 1/*f* noise from the active region can be measured under bias currents far lower than the threshold currents of the LDs, and it can indicate the defects in the active region and further the reliability of the device.

1. Introduction

With the development of electrooptical technology, semiconductor LDs are fulfilling various complex environments and actual demands due to the advantages including small size, long lifetime, selectable wavelength and convenient integration [1–8]. During the recent decades, new breakthroughs are constantly achieved with the deeper understanding on the LD structure and the electrical characteristics, such as double heterojunction LDs, quantum well LDs and so on, which not only enhance the power of semiconductor LDs but also give them advantages including low threshold current, good temperature stability and high photoelectric conversion efficiency [1–5]. At present, the power LDs aiming at enhancing the luminous power are one of the major research field. For high-power semiconductor LDs, how to enhance the power, lifetime and reliability is of great research worthiness [6–8].

1/*f* noise, as a colored noise, is a nonstationary stochastic process that exists broadly in all kinds of electronic devices [9–11]. Some researches consider the noise generation mechanism related to the density and motion parameters of the internal particles [12,13]. There are different models based on the carrier density or the mobility fluctuation or the unification of both [14], and the most well accepted cause is the interface-trap-induced charge-carrier-fluctuation theory [15,16]. As the existing theoretical models usually apply only to some certain devices, the research on the characteristics of 1/*f* noise is still a potential hot topic [17–19]. Especially in recent years the researchers find that there is a close relationship between 1/*f* noise and the reliability and lifetime of the semiconductor devices, so the 1/*f* noise measurement and characteristic analysis can be used as an effective nondestructive testing method to evaluate the property and reliability [20–22].

The traditional LD reliability examinations are mostly conducted by electric aging tests [7], which is a destructive testing method. Especially for the high-power semiconductor LDs, due to the high threshold current, long-time testing under high current will exacerbate the active region material surface defects, and severely damage the device internal structure. Therefore, it is meaningful to investigate a non-destructive testing method, especially the device characteristics under bias currents far below its threshold current [23]. There is a close connection between the LD bias currents and their photoelectric and 1/*f* noise characteristics [24–30], and if the 1/*f* noise from different origins of the high-power devices can be measured under the bias far below their threshold currents, that would be very helpful for the non-destructive testing. In this experiment, the devices are tested under various currents below one tenth the threshold current of the high-power semiconductor LDs to measure the noise power spectrum density (PSD), including the voltage PSD and

* Corresponding author.
E-mail address: gaofl@jlu.edu.cn (F. Gao).

http://dx.doi.org/10.1016/j.microrel.2015.12.029
0026-2714/

current PSD, and the PSD intensities at 20 Hz are extracted to indicate the relationship between the noise intensity and the bias currents, which are used to analyze the working conditions of the LDs and their noise origins. Meanwhile, with the voltage–current and electrical derivative (IdV/dI) characteristics, the noise origins are verified from different angles, and the internal defect degree and reliability of the devices are analyzed.

2. Experiment and method

The schematic of experimental measurement system is shown in Fig. 1. As in the figure, the dash box indicates the 9812D system (ProPlus, USA) for the current $1/f$ noise measurement, where the IV Meter 4156C (Agilent, USA) powers the LD samples and measures their voltage–current (V–I) characteristics. The current $1/f$ noise signals are collected, amplified and fast-Fourier transformed by 9812D, and the results are processed and plotted by a computer. The rest of Fig. 1 is the voltage $1/f$ noise measuring system we build on our own, where the bias control circuit consists of a 12 V accumulator and some slide rheostats to power the samples and adjust the bias current. The circuit and the samples are set in a customized low-frequency shielding box. The ampere meter (Model 3458A, Agilent, USA) is used to monitor the bias current and shorted when the noise is measured. The voltage noise signals are amplified by a pre-amplifier (Model 5184, AMETEK, USA) and input into the spectrum analyzer (CF-9200, Onosokki, Japan) to acquire the noise power spectrum density. The voltage and current $1/f$ noise should meet the Ohm's law, which can indicate the accuracy of the measurement results. The experimental samples are InGaAs quantum well high-power LDs manufactured by the 13th Research Institute of China Electronics Technology Group Corporation. The sample power is 3 W, the laser wavelength is 976 nm, the cavity length is 2000 μm, the quantum well width is 10 nm and the threshold current is 300 mA.

Within the current range under the threshold current, the V–I characteristic of the LDs can be approximately modeled as the typical diodes, the simplified equivalent circuit shown in Fig. 2, mainly consisted of the PN junction dynamic resistance R_a, contact resistance R_c and leakage resistance R_p [4]. The voltage–current equation is shown as below

$$I = I_s\left(\exp(qV_j/mkT) - 1\right) + I_p \tag{1}$$

$$V = (I - I_p)R_c + V_j \tag{2}$$

where I is the total bias current, I_p is the leakage current, I_s is the reverse saturation current, V_j is the forward junction voltage, q is the electron charge, m is the extrinsic factor, k is the Boltzmann constant and T is the absolute temperature. Under a forward voltage, $\exp(qV_j/mkT) \gg 1$,

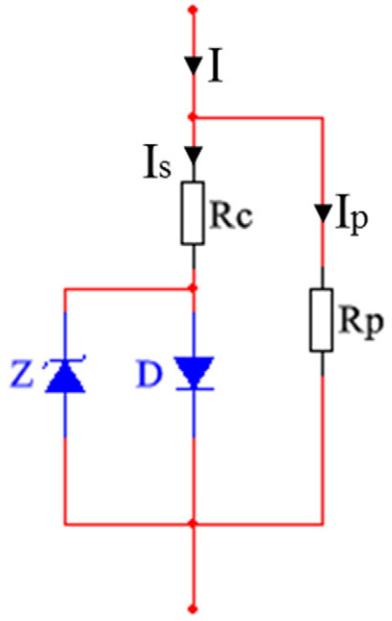

Fig. 2. The simplified equivalent circuit of LDs.

so according to Eqs. (1) and (2), ignoring R_p the relationship between the dynamic resistance and the bias current is as below

$$R = \frac{dV}{dI} = R_c + \frac{mkTI_s}{q(I - I_p)}. \tag{3}$$

From Eq. (3) we can see that the resistance is much higher under very low bias current and declines very fast in inverse proportion with the current increasing.

$1/f$ noise is the low frequency noise that exists broadly in electronic devices. According to Fig. 2, the major noise origins are the active region dynamic resistance, the contact resistance, and the leakage resistance. According to the equivalent circuit and the Hooge empirical formula [13], the voltage $1/f$ noise can be described as below

$$S_V(f) = \frac{\alpha}{N_p f}{R_p}^2{I_p}^2 + \left(R_c + \frac{mkTI_s}{q(I - I_p)}\right)^2 \frac{2}{3}\alpha\frac{q(I - I_p)}{f\tau_n} + \frac{\alpha}{N_c f}{R_c}^2(I - I_p)^2 \tag{4}$$

where N_p is the total carrier density in the leakage resistance, N_c is the total carrier density in the contact resistance and α is the Hooge

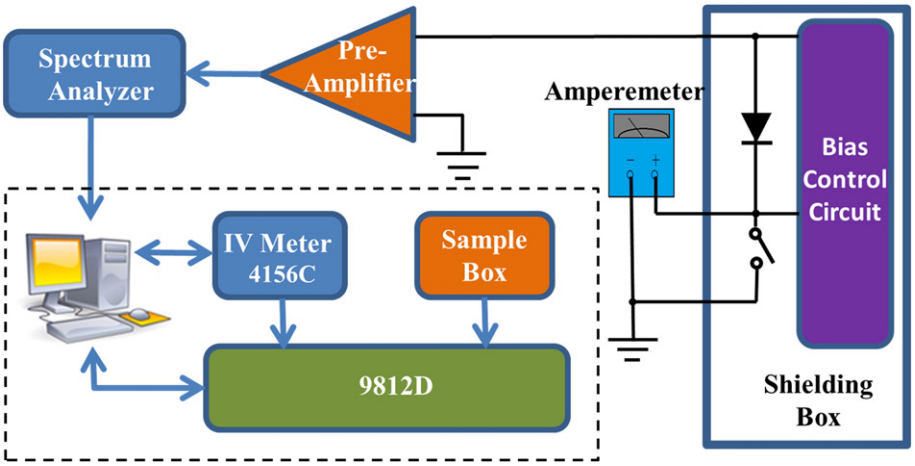

Fig. 1. The $1/f$ noise measurement system sketch.

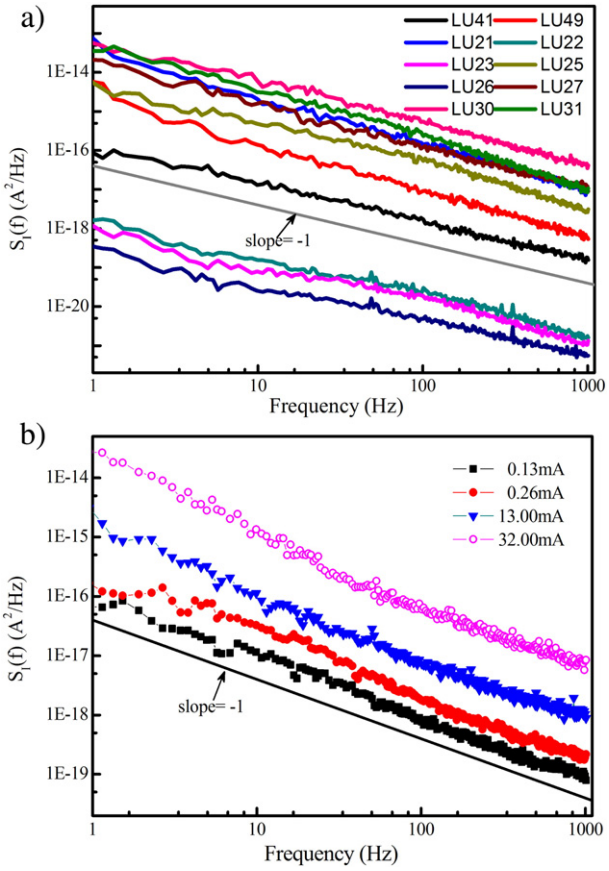

Fig. 3. The 1/*f* noise PSDs. (a) Different samples under 0.26 mA. (b) LU41 under different bias currents.

constant decided by the material. In Eq. (4) the first term represents the noise from the leakage resistance, the second term represents the noise stimulated by the diffusion current fluctuation caused by the interface trap in the active region, and the third represents the noise from the contact resistance. Therefore, the major noise origins under different bias currents can be analyzed with the quantitative relations of the voltage noise, current noise and the dynamic resistance.

3. Measurement results and discussion

About 50 functional samples are tested for their 1/*f* noise and electrical characteristics. All the results present typical 1/*f* noise features, and

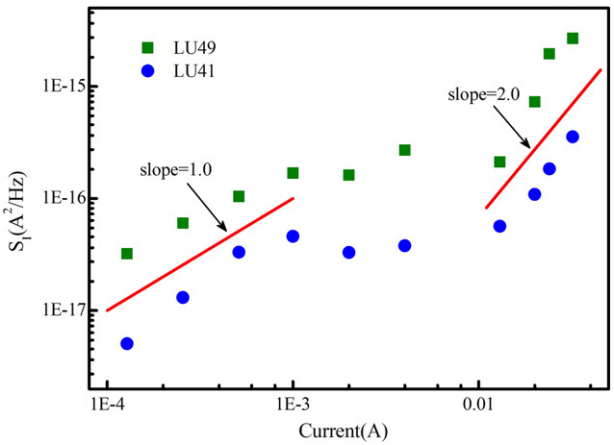

Fig. 4. The current 1/*f* noise PSD (20 Hz) of the two devices under different bias currents.

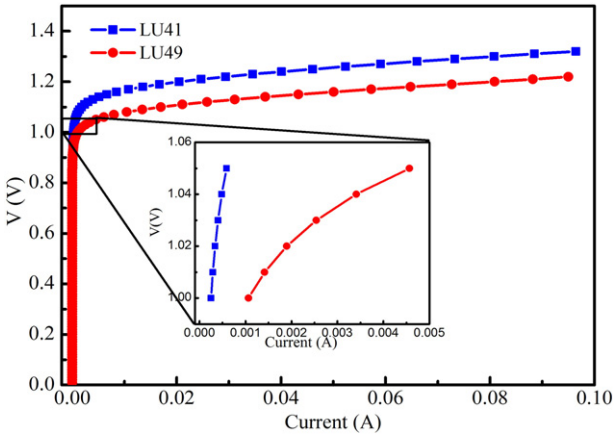

Fig. 5. The V–I correlations of the two LDs.

the differences are mainly reflected in the noise intensities. The current 1/*f* noise PSDs of part of the samples are shown in Fig. 3, in which Fig. 3(a) is the PSDs of different samples under 0.26 mA and Fig. 3(b) is LU41 under four different bias currents 0.13 mA, 0.26 mA, 13 mA, and 32 mA. From Fig. 3 we can see that in this frequency band, the low frequency noise of the LDs shows typical 1/*f* noise features. Compared with the *slope* = −1 reference line, the PSD curves are basically stable and parallel, which indicates that the noise component in this frequency range mainly consists of pure 1/*f* noise. Next we use the PSD values at 20 Hz to further investigate the 1/*f* noise characteristics under low bias currents. The results of different samples present similar regularity, so we choose two typical results, LU41 and LU49, for demonstration.

The S_I-I curves of LU41 and LU49 are shown in Fig. 4, where S_I represents the PSD values at 20 Hz. From Fig. 4, we can see the current 1/*f* noise intensities change closely related to the bias current, and the changing patterns are almost identical. In the current range between 0.13 mA and 1 mA, the curves show a *slope* ≈ 1 linear correlation in the logarithm coordinate. From the Eq. (3) and the second term in Eq. (4), we know that the current 1/*f* noise from the active region is in proportion to the bias current. Therefore, we primarily consider that the 1/*f* noise in this bias current range is from the active region. In addition, from Fig. 4 we can see that the noise level of LU49 is one order larger than LU41, which indicates that there are more internal defects created during the manufacture of LU49 than LU41 [27], especially in the active region which is closely related to the reliability of LDs. Additionally, we can also observe that the curves flatten between 1 mA and 8 mA. This is because with the bias current increasing, more carriers are injected into the active region, which causes the recombination of

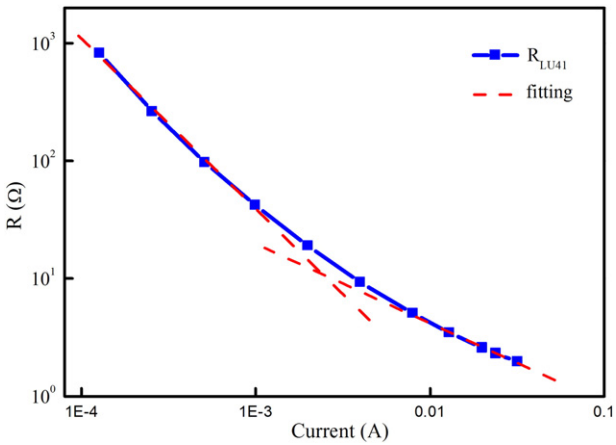

Fig. 6. The dynamic resistance curve of LU41.

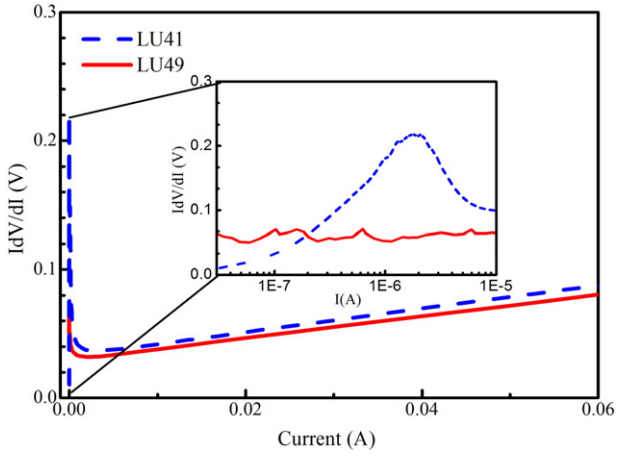

Fig. 7. The electrical derivative curves of LU41 and LU49.

the carriers and traps in the active region increasing, but meanwhile the carrier concentration in the series resistor is declining, so the current diffusion to the active region is suppressed [31], the two aspects above cause that the 1/*f* noise intensity hardly changes with the bias current.

The electrical characteristics are also an important factor in analyzing the performance of the LDs [23,25,28–30], in order to establish the connection between the electrical characteristics and 1/*f* noise, the voltage–current (V–I) correlations of the LDs are shown in Fig. 5. We can see that both devices conform to the typical V–I characteristics of LDs, and from the inset, the two LDs show obvious differences in a rather low bias current range, but the V–I characteristics are not quantitatively explicit to demonstrate the noise origins and the differences between the LDs, so the dynamic resistance and electrical derivative are computed to further analyze the connection between the electrical characteristics and 1/*f* noise.

The dynamic resistance and electrical derivative of LU41 are computed from Fig. 5 and Eq. (3), as shown in Figs. 6 and 7. From Fig. 6, we can see that under the bias currents form 0.13 mA to 1 mA, the LD dynamic resistance is at the magnitude of hundreds of ohms, far higher than the contact resistance. Moreover, it is also in a diminishing linear correlation with the bias current in the logarithm coordinate, corresponding to the active region dynamic resistance feature in Eq. (3), which indicates that the major voltage drop is on the active region and further verifies that the active region is the major 1/*f* noise origin under these bias currents. With the bias current increasing, a nonlinearity correlation with the dynamic resistance is gradually reflected and when the bias current is larger than 8 mA the dynamic resistance drops to less than 10 Ω. Meanwhile, from Fig. 4 we can also see that the noise intensity enhances rapidly, and shows a *slope* ≈ 2 linear correlation, which illustrates that contact resistance is gradually dominating the LD dynamic resistance according to the third term in Eq. (4), so its voltage drop is occupying most of the bias voltage and the contact resistance R_c becomes the dominating 1/*f* noise origin.

The factors such as internal defect, cavosurface damage and surface leakage current cause the interface traps stochastically capturing and releasing the carriers, and leads to tiny current fluctuation [15,16], which for LDs we suppose it will influence the electrical derivative under extremely low bias currents. The derivative is closely related to the reliability of LDs [30,31], and for the purpose of further investigating the relationship between the difference of the two LDs' noise intensity and their reliability, the electrical derivative curves of LU41 and LU49 are shown in Fig. 7, where the detailed curves near the initial peaks are shown in the inset. From Fig. 7 we can see that the two curves have a similar trend in the whole current range, but are obviously different near their initial peaks. As the inset shows, the initial peak of LU41 is more distinguishable, and the electrical derivative curve is smoother near the peak, while the LU49 electrical derivative curve does not show an obvious initial peak, and fluctuates continually. This phenomenon indicates that the current fluctuation in LU41 is much milder than LU49 under the extremely low driving current, so the factors influencing the reliability of LU41 are better than LU49, which conforms to the feebler 1/*f* noise of LU41 as shown in Fig. 4. The comparison between initial peak fluctuation and noise intensity (0.26 mA, 20 Hz) of the ten samples in Fig. 3 are listed in Table 1, from which we can see that the results are coherent to the former analysis. The existence of noise is equivalent to a weak leakage mechanism added to the ideal physical model (Fig. 2), which can be considered in parallel with R_p and changes the leakage characteristics of the sample. The initial peak is caused by the co-effect of the leakage resistance and active region and appears under extremely low bias current. Therefore the 1/*f* noise as a weak current fluctuation influences the initial peak distinctly. However, as shown in Fig. 7, this influence does not exhibit an obvious pattern with the bias current changing, which can only reflect the existence of these factors, whereas the 1/*f* noise aroused by them is reflected in a wider current range and shows a distinct regularity, as shown in Figs. 3 and 4.

In order to further investigate the noise origin between 0.13 mA and 1 mA, the voltage 1/*f* noise PSD is measured at the same time, and combining the dynamic resistance at the corresponding bias currents, the S_I values are also computed by Ohm's law $S_I = S_V/R^2$. According to Eq. (4), if the noise signal acquired is originated by the active region, its S_V curve will show a linear diminishing trend with the bias current growing in the logarithm coordinate. The results of LU41 are shown in Fig. 8, where S_I and S_V are the current voltage PSD values at 20 Hz. We can see that S_V curve conforms to the former analysis, meanwhile the trend of the computed S_I is in fine coherence with the measured S_I, which also confirms the accuracy of former measurements. The amplitude difference attributes to the different gains between Model 5184 and the pre-amplifier in 9812D. Therefore, we can further conclude that the major origin of the 1/*f* noise in this current range is the active region.

The traditional stress process to examine the reliability of LDs creates defects in both the active region and the contact resistance and brings enhancement to the 1/*f* noise, especially in the active region [27]. From our experiments, under a very low range of bias current, the 1/*f* noise of high-power LDs from both origins can be measured, so the 1/*f* noise measurement of high-power LDs under low bias currents is conducive to the nondestructive evaluation of their reliability.

4. Conclusion

The factors such as the internal defects, cavosurface damage and surface leakage current are highly related to the reliability of high-power LDs, and influence the 1/*f* noise and electrical characteristics of the devices. In our experiments, under very low bias currents, we acquire the 1/*f* noise from different origins of the high-power LDs. Under less than 1/10 the threshold current, the low frequency noise PSD of the tested devices shows typical 1/*f* noise features, and the relationships between the noise intensity and the bias currents of different devices

Table 1
Comparison between the initial peak fluctuation (IPF) and noise intensity (NI) (0.26 mA, 20 Hz) of the ten samples.

LD No.	LU21	LU22	LU23	LU25	LU26	LU27	LU30	LU31	LU41	LU49
IPF	Acute	Smooth	Smooth	Strong	Smooth	Acute	Acute	Strong	Smooth	Strong
NI (A^2/Hz)	1.01E−15	7.5E−20	4.8E−20	3.3E−16	1.9E−20	5.8E−16	2.8E−15	1.6E−15	7.9E−18	6.0E−17

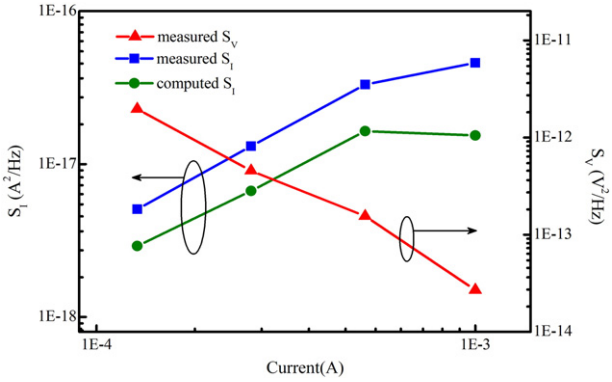

Fig. 8. The current and voltage 1/*f* noise comparison.

show a consistent pattern. The results of the 1/*f* noise measurements demonstrate that the 1/*f* noise from the active region can be acquired with the bias currents far below the threshold current, and with the bias current increasing the major origin of the 1/*f* noise is dominated by the contact resistance. Besides, the voltage 1/*f* noise PSD and the relationship between the dynamic resistance and the bias current also confirm the noise origin analysis. Additionally, as for the difference between the 1/*f* noises of the two LDs, the electrical derivative curves show that the LD with higher 1/*f* noise has acuter derivative fluctuation and no obvious initial peak. In conclusion, for high-power LDs, the 1/*f* noise from the active region can be measured with bias currents far below the threshold current, so we believe that the 1/*f* noise measurement of high-power LDs under low current range is a practical solution to the reliability evaluation of the devices. In our future researches, we plan to investigate more precise correlation between 1/*f* noise and the derivative of LDs to build their quantitative model.

Acknowledgment

This work is financially supported by the Young Scientists Fund of the National Natural Science Foundation of China (Grant No. 61204055), National Key Scientific Instrument and Equipment Development Project of China (Grant No. 2011YQ040077), and the Young Science and Research Fund (Grant No. 20130522188JH) and the Natural Science Foundation of Jilin Province of China (Grant No. 20140101175JC).

References

[1] L. Riuttanen, P. Kivisaari, H. Nykänen, et al., Diffusion injected multi-quantum well light-emitting diode structure, Appl. Phys. Lett. 104 (2014) 081102.
[2] C. De Santi, M. Meneghini, M. Marioli, et al., Thermally-activated degradation of InGaN-based laser diodes: effect on threshold current and forward voltage, Microelectron. Reliab. 54 (2014) 2147–2150.
[3] M. Haas, A. Killi, C. Tillkorn, et al., Thin-film filter, wavelength-locked, multi-laser cavity for dense wavelength beam combining of broad-area laser diode bars, Opt. Lett. 40 (2015) 3949–3952.
[4] M.F. Lu, J.S. Deng, C. Juang, et al., Equivalent circuit model of quantum-well lasers, IEEE J. Quantum Electron. 31 (1995) 1418–1422.
[5] D.F. Welch, A brief history of high-power semiconductor lasers, IEEE J. Sel. Top. Quantum Electron. 6 (2000) 1470–1477.
[6] Y. Qu, S. Yuan, C.Y. Liu, et al., High-power InAlGaAs/GaAs and AlGaAs/GaAs semiconductor laser arrays emitting at 808 nm, IEEE Photon. Technol. Lett. 16 (2004) 389–391.
[7] H. Zhu, K. Liu, C. Xiong, et al., The effect of external stress on the properties of AlGaAs/GaAs single quantum well laser diodes, Microelectron. Reliab. 55 (2015) 62–65.
[8] Y. Liu, S. Zhao, S. Yang, et al., Markov process based reliability model for laser diodes in space radiation environment, Microelectron. Reliab. 54 (2014) 2735–2739.
[9] A.A. Balandin, Low-frequency 1/*f* noise in graphene devices, Nat. Nanotechnol. 8 (2013) 549–555.
[10] F.N. Hooge, 1/*f* noise sources, IEEE Trans. Electron Devices 41 (1994) 1926–1935.
[11] Y. Lai, H. Li, D.K. Kim, et al., Low-frequency (1/*f*) noise in nanocrystal field-effect transistors, ACS Nano 8 (2014) 9664–9672.
[12] E. Paladino, Y.M. Galperin, G. Falci, et al., 1/*f* noise: implications for solid-state quantum information, Rev. Mod. Phys. 86 (2014) 361.
[13] F.N. Hooge, The relation between 1/*f* noise and number of electrons, Physica B 16 (1990) 344–351.
[14] T.H. Morshed, S.P. Devireddy, Z. Celik-Butler, et al., Physics-based 1/*f* noise model for MOSFETs with nitrided high-κ gate dielectrics, Solid State Electron. 52 (2008) 711–724.
[15] Z. Celik-butler, T.Y. Hsiang, Determination of Si-SiO_2 interface trap density by 1/*f* noise measurements, IEEE Trans. Electron Devices 35 (1988) 1651–1655.
[16] D.M. Fleetwood, J.H. Scofield, Evidence that similar point defects cause 1/*f* noise and radiation-induced-hole trapping in metal–oxide–semiconductor transistors, Phys. Rev. Lett. 64 (1990) 579.
[17] G. Liu, S. Rumyantsev, M.S. Shur, et al., Origin of 1/*f* noise in graphene multilayers: surface vs. volume, Appl. Phys. Lett. 102 (2013) 093111.
[18] S.J. Heerema, G.F. Schneider, M. Rozemuller, et al., 1/*f* noise in graphene nanopores, Nanotechnology 26 (2015) 074001.
[19] M. Niemann, H. Kantz, E. Barkai, Fluctuations of 1/*f* noise and the low-frequency cutoff paradox, Phys. Rev. Lett. 110 (2013) 140603.
[20] S. Pralgauskaitė, V. Palenskis, J. Matukas, et al., Reliability investigation of light-emitting diodes via low frequency noise characteristics, Microelectron. Reliab. 55 (2015) 52–61.
[21] L.Z. Hasse, S. Babicz, L. Kaczmarek, et al., Quality assessment of ZnO-based varistors by 1/*f* noise, Microelectron. Reliab. 54 (2014) 192–199.
[22] P. Del Vecchio, A. Curutchet, Y. Deshayes, et al., Correlation between forward–reverse low-frequency noise and atypical I–V signatures in 980 nm high-power laser diodes, Microelectron. Reliab. 55 (2015) 1741–1745.
[23] D. Li, H. Zong, W. Yang, et al., Stimulated emission in GaN-based laser diodes far below the threshold region, Opt. Express 22 (2014) 2536–2544.
[24] B.K. Jones, Electrical noise as a reliability indicator in electronic devices and components, IEE Proc. Circ. Devices Syst. 149 (2002) 13–22.
[25] J. Al Roumy, J. Perchoux, Y.L. Lim, et al., Effect of injection current and temperature on signal strength in a laser diode optical feedback interferometer, Appl. Opt. 54 (2015) 312–318.
[26] A. Van der Ziel, Unified presentation of 1/*f* noise in electron devices: fundamental 1/*f* noise sources, Proc. IEEE 76 (1988) 233–258.
[27] X.Y. Chen, A. Pedersen, A.D. Van Rheenen, Effect of electrical and thermal stress on low-frequency noise characteristics of laser diodes, Microelectron. Reliab. 41 (2001) 105–110.
[28] D. Guo, L. Cheng, X. Chen, et al., Electrical derivative measurement of quantum cascade lasers, J. Appl. Phys. 109 (2011) (043105-043105-3).
[29] Q. Liyun, S. Jiawei, L. Hongyan, et al., The peaks in the electric derivative curves and optic derivative curves of GaAs/GaAlAs high-power QW lasers, Microelectron. Reliab. 40 (2000) 2123–2128.
[30] P.A. Barnes, T.L. Paoli, Derivative measurements of the current–voltage characteristics of double-heterostructure injection lasers, IEEE J. Quantum Electron. 12 (1976) 633–639.
[31] C.M. Wu, E.S. Yang, Current suppression induced by conduction-band discontinuity in $Al_{0.35}Ga_{0.65}As$–GaAs N–p heterojunction diodes, J. Appl. Phys. 51 (1980) 2261–2263.